# Slow Mass Transport and Statistical Evolution of an Atomic Gas across the Superfluid–Mott-Insulator Transition

Chen-Lung Hung, Xibo Zhang, Nathan Gemelke, and Cheng Chin

*The James Franck Institute and Department of Physics, The University of Chicago, Chicago, Illinois 60637, USA*

We study transport dynamics of ultracold cesium atoms in a two-dimensional optical lattice across the superfluid-Mott-insulator transition based on *in situ* imaging. Inducing the phase transition with a lattice ramping routine expected to be locally adiabatic, we observe a global mass redistribution which requires a very long time to equilibrate, more than 100 times longer than the microscopic time scales for on-site interaction and tunneling. When the sample enters the Mott-insulator regime, mass transport significantly slows down. By employing fast recombination loss pulses to analyze the occupancy distribution, we observe similarly slow-evolving dynamics, and a lower effective temperature at the center of the sample.

The thorough understanding of atomic interactions in optical lattices provides a testing ground to investigate hypothetical models widely discussed in condensed matter and many-body physics [1,2]. Because of the simplicity and tunability of the underlying Hamiltonian, research on optical lattices generates new fronts to perform precise, quantitative comparison between theoretical calculations and measurements. This new class of "precision many-body physics" has generated tremendous interest in recent years to locate the superfluid (SF) to Mott-insulator (MI) phase boundaries [3–5], described by the Bose-Hubbard model [6,7], and to characterize Mott and band insulators in Fermi gases [8,9], described by the Fermi-Hubbard model [10]. Many new, exotic quantum phases in optical lattices have also been proposed [2], even in the absence of counterparts in condensed matter physics.

As promising as the precise characterization of quantum phases is, fundamental assumptions such as the thermodynamic equilibrium of the sample should be investigated. Since the preparation of quantum gases generally involves ramping up the lattice potential, dynamics are an inseparable part of all optical lattice experiments. Very slow equilibration processes have been reported in one-dimensional optical lattices [11] and have been suggested by the observation of long-lived repulsively bound pairs [12] and doublons [13] in three-dimensional lattices. Prospects of nonequilibrium dynamics in optical lattices have also attracted much interest recently. Mass and entropy transport in the optical lattices can provide a wealth of information to characterize the underlying quantum phases [14,15]. Dynamic passage across a phase transition can lead to the proliferation of topological defects in the optical lattices [16].

In this Letter, we study global dynamics of ultracold atomic gases in a monolayer of two-dimensional (2D) optical lattice. After ramping up the lattice potential, we observe both mass transport and statistical distribution of atomic occupancy in the lattice. Mass transport is directly

seen from *in situ* density profiles, while occupancy statistics is probed by inducing loss in sites of three or more atoms using a fast three-body recombination loss pulse (see Fig. 1). Both processes show intriguing behavior at times much longer than microscopic time scales for atomic interaction and tunneling.

We begin the experiment with a $^{133}$Cs quantum gas in a 2D optical trap. Details on the preparation of the quantum gas and optical lattice loading procedure can be found in Refs. [17,18], respectively. In brief, a nearly pure Bose
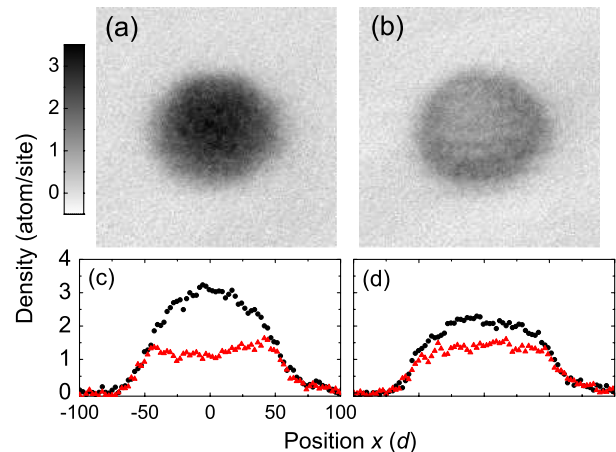


FIG. 1 (color online).　Averaged absorption images and density cross sections of $N = 2 \times 10^4$ cesium atoms in a monolayer of 2D optical lattice. After ramping the lattice in 150 ms to a lattice depth $V_f = 13E_R$, (a) shows the sample immediately after the ramp. In (b), an additional fast recombination pulse removes atoms in sites of occupancy three or more. (c) shows the average density cross sections of (a) (circles) and (b) (triangles). (d) shows the average density cross sections of the samples with additional 800 ms hold time after the ramp, without (circles) and with the recombination loss pulse (triangles). Image size is $(106 \ \mu m)^2 = (200 \ \text{sites})^2$ and seven images are used in each averaged result.

condensate is loaded into a 2D optical dipole trap, formed by two orthogonally crossed beams on the $x$-$y$ plane and a one-dimensional vertical optical lattice of 4 $\mu$m spacing which confines the whole sample in a single "pancake-like" lattice site [18]. Using microwave tomography, we find ∼95% of the atoms are loaded into a single pancake trap. The remaining ∼5% in the neighboring sites do not contribute to the main results reported in this letter. The trap vibration frequencies are $(\omega_x, \omega_y, \omega_z) = 2\pi \times (11, 13, 1970)$ Hz, and the cloud temperature is $T = 11$ nK. The ratios $\hbar\omega_i/k_B T = (0.05, 0.06, 9)$ indicate the sample is two dimensional. After 2D trap loading, we adjust the atomic scattering length $a$ by ramping the magnetic field to a designated value, typically, $B = 20.7$ G, where $a = 200a_B$ and $a_B$ is the Bohr radius. At this field, the three-body recombination loss rate is at the Efimov minimum [19].

We introduce a 2D optical lattice by slowly turning on retro-reflections of the crossed dipole beams which add a square lattice potential with lattice spacing $d = 532$ nm and a weak contribution to the envelope confinement characterized by a mean radial frequency $\sqrt{\omega_x\omega_y} = 2\pi(1 + V/82E_R) \times 12$ Hz, where $E_R = k_B \times 64$ nK is the recoil energy and $V$ is the lattice depth. Care is taken to equalize lattice depths in the $x$ and $y$ directions by balancing the lattice vibration frequencies to within 5%. Based on the vibration frequency measurements, we calculate tunneling $t$ and on-site interaction $U$ numerically from the band structure in a homogeneous 2D lattice.

We ramp on the lattice depth following $V(\tau) = V_f(1 + \gamma)/[1 + \gamma e^{4(\tau - \tau_c)^2/\tau_c^2}]$ [20], preceded by a 30 ms linear ramp from 0 to 0.4 $E_R$ to ensure a smooth turning on of the lattice potential at low depth. The final depth $V_f$ is reached at time $\tau = \tau_c$ and $\gamma$ is chosen such that $V(0) = 0.4E_R$. After the ramp, the sample is held in the lattice for a hold time $\tau_{\text{hold}}$. The adiabaticity parameter of the ramp is given by $\alpha = \hbar|\dot{t}|/t^2$; slow ramps with $\alpha < 1$ suggest that local equilibrium of the system is preserved [20,21].

We obtain the *in situ* density profile of the sample by absorption imaging normal to the $x$-$y$ plane. After a hold time $\tau_{\text{hold}}$, we first switch the magnetic field to $B = 17.7$ G ($a = 40a_B$) and then turn off the 2D lattice 100 $\mu$s before the imaging, reducing the on-site peak density by a factor of 30, in order to mitigate any density dependent loss during the imaging process [22]. The atomic density is measured with a spatial resolution of 1.3 $\mu$m using a long working distance (34 mm) commercial microscope objective. The strength and duration of the imaging pulse are chosen to keep the travel distance of the atoms due to the radiation pressure from the imaging beam small compared to the depth of focus, while maintaining a good signal-to-noise ratio.

Our first step to study the global dynamics is to watch how the density profile equilibrates after a lattice ramp. Here we employ a ramp which is locally adiabatic, but is

fast enough to induce detectable mass flow. An example is shown in Fig. 2(a), where after a $\tau_c = 20$ ms ramp to $V_f = 10E_R$ ($U/t = 11$, $\alpha < 0.6$) the sample of $N = 2 \times 10^4$ atoms at scattering length $a = 200a_B$ gently expands and the peak density slowly decreases. This deformation is consistent with the increase of repulsive atomic interaction in stronger lattice confinement.

To quantify the rate of mass redistribution, we define the root-mean-square deviation of a density profile at hold time $\tau$ from equilibrium as $\Delta(\tau) = \{\sum_i[\bar{n}_i(\tau) - \bar{n}_{\text{eq},i}]^2\}^{1/2}$, where the sum goes over lattice sites enclosing the sample. $\bar{n}_i(\tau)$ is the mean occupancy of site $i$ at hold time $\tau$, obtained by averaging over an annular area centered on the cloud, containing site $i$, and with width 1.3 $\mu$m [18]. $\bar{n}_{\text{eq},i}$ is the mean occupancy of site $i$ at equilibrium, which we obtain from samples that cease to evolve after long hold time of $\tau_{\text{hold}} = 500$–$800$ ms.

At lattice depths $V_f < 10E_R$, the sample shows a weak breathing mode oscillation in the first 50 ms of hold time. After 50 ms, $\Delta(\tau)$ can be fit by single exponential decays with time constants $>100$ ms. When the lattice depth reaches $11E_R$ or higher, the mass flow slows down significantly, see Figs. 2(b) and 2(c), suggesting that the mass transport is suppressed in this regime. The crossover behavior near $V_f = 11E_R$, where $U/t \approx 15$, is consistent with a recent observation of the suppression of superfluidity at $U/t = 16$ in a 2D optical lattice [5], and quantum Monte Carlo calculations, predicting that the SF-MI transition at the tip of the $n = 1$ Mott lobe occurs
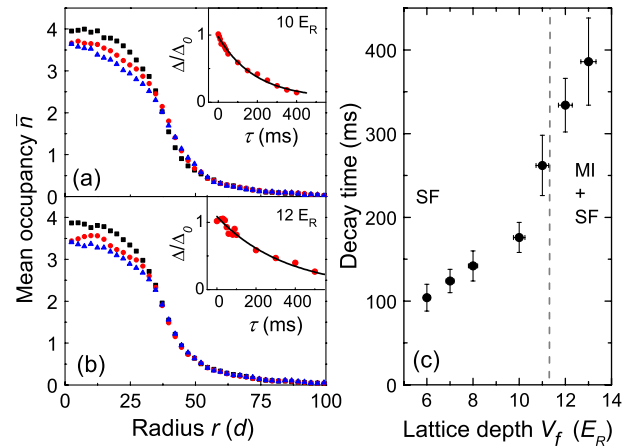


FIG. 2 (color online). Evolution of the density profile after a short lattice ramp. Following a $\tau_c = 20$ ms ramp to $V_f = 10E_R$ ($U/t = 11$, $\alpha < 0.6$), (a) shows the radial density profiles measured after hold times of 0 (squares), 200 (circles), and 500 ms (triangles). Inset shows the time evolution of $\Delta$, normalized to the initial value $\Delta_0 = \Delta(0)$ (circles) and the single exponential fit. (b) shows the profiles measured at $V_f = 12E_R$ ($U/t = 20$, $\alpha < 1$). The fitted decay times at different depths of $V_f$ are shown in (c), where the dashed line marks the critical lattice depth, see text.

at $U/t \approx 16.74$ in 2D [24]. For $V_f > 13E_R$, even slower dynamics require much longer hold time and the slow loss from three-body recombination limits our ability to determine the mass redistribution time scale [25].

The slow dynamics throughout the SF-MI regime indicate that the global thermalization is much slower than the microscopic time scales. Indeed, in the range of $V_f = 6$–$13E_R$, tunneling to neighboring sites occurs in $\tau_t = \hbar/zt = 0.6$–$3$ ms, where $z = 4$ is the coordination number of the 2D square lattice.

In the second experiment, we investigate the evolution of occupancy statistics. For this, we develop a scheme to determine the fraction of sites with three or more atoms by inducing a fast three-body recombination loss, and comparing the density profiles with and without the loss. For cesium atoms, extremely fast three-body loss can be induced by jumping the magnetic field near an Efimov resonance [19], where the loss happens much faster than atoms tunnel.

We induce the recombination loss at $V_f = 13E_R$ by jumping the magnetic field to $B = 2$ G for a duration of 1 ms before imaging at 17.7 G. The $1/e$ time of the field switching is below $100$ $\mu$s. During the switching, the magnetic field from the eddy currents is measured by microwave spectroscopy and compensated by a controlled overshoot of currents in the magnetic coils. At 2 G, the three-body loss rate is as high as $(20\ \mu s)^{-1}$ for 3 atoms in one site, much faster than the tunneling rate $1/\tau_t = (3\ \text{ms})^{-1}$, and the 1 ms pulse is sufficient to remove all the atoms that could participate in the loss process.

We analyze the dynamics of on-site statistics by first ramping the lattice in $\tau_c = 300$ ms to $V_f = 13E_R$ ($U/t = 41$, $\alpha < 0.1$) at scattering length $a = 310a_B$ and then holding the sample for up to 800 ms. Here, the lattice ramp is slow enough to ensure negligible subsequent mass flow. Density profiles at different hold times, with and without the loss pulse, are shown in Figs. 3(a)–3(c). A larger fractional loss occurs at the central part of the sample where the density is higher, as expected; there is no apparent loss in the wing. We observe a smaller fractional loss after a longer hold time, which suggests that fewer sites are found with three or more atoms.

The evolution of the statistics is best shown in Fig. 3(d), where the atom loss, $\Delta\bar{n}$, is induced by the recombination pulse after different hold times. A dramatic difference is seen near the center with mean occupancy near $\bar{n} = 2$. Here the loss fraction reaches $\Delta\bar{n}/\bar{n} = 50\%$ immediately after the ramp, and it slowly declines to merely 15% after a hold time of $\tau_{\text{hold}} = 800$ ms.

To quantitatively model the loss, we assume, starting with $n$ atoms in one site, ($n$ modulo 3) atoms remain after the pulse. To test this model, we prepare an ideal 2D gas by tuning the magnetic field to $B = 17.1$ G, where $a \approx 0a_B$. We then quickly ramp on the lattice to $30E_R$ in 10 ms to freeze the on-site occupancy and perform the loss mea-
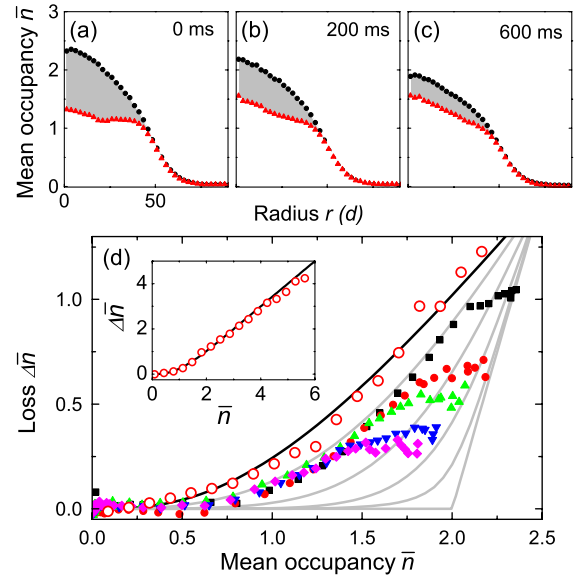


FIG. 3 (color online).    Evolution of the on-site statistics in a Mott insulator. ($N = 1.6 \times 10^4$, $\tau_c = 300$ ms, $V_f = 13E_R$). Upper figures show the density profiles of the samples held in the final depth $V_f = 13E_R$ for $\tau_{\text{hold}} = $ (a) 0, (b) 200, (c) 600 ms and then imaged with (triangles) and without (circles) the recombination pulse. Shaded areas mark the loss fractions. (d) shows the loss $\Delta\bar{n}$ versus mean occupancy $\bar{n}$ measured after different hold times (filled symbols): 0 (squares), 200 (circles), 400 (upward triangles), 600 (downward triangles), and 800 ms (diamonds). Gray lines are the loss derived from an insulator model, see text, assuming $k_B T/U = 1$ (higher curve), 0.5, 0.3, 0.2, and 0 (lower curve). The black line, derived from the Poisson distribution, is in good agreement with an ideal gas measurement (open circles). The inset shows an extended view.

surement. For noninteracting particles, we expect the occupancy obeys a Poisson distribution. The calculated atom loss see black solid lines in Fig. 3(d) and the inset, is in good agreement with our measurement.

Recombination losses measured with interacting samples and slow lattice ramps, on the other hand, deviate from the Poisson model toward lower values for all mean occupancies [see Fig. 3(d)]. This is a general characteristic of the strongly interacting gas.

To gain further insight into the occupancy statistics in an insulator we compare our measurement with an analytic model based on a grand canonical ensemble [26,27]. In deep lattices with $t \ll U$, $k_B T$, the probability for occupancy $n$ can be written as $P_n = Q^{-1}e^{-\beta(H_n - \mu n)}$, where $H_n \approx (U/2)n(n-1)$, $\beta = 1/k_B T$, $\mu$ is the local chemical potential and $Q = \sum_n e^{-\beta(H_n - \mu n)}$ is the grand partition function. The mean occupancy is then $\bar{n} = \sum n P_n$ and the loss is modeled as $\Delta\bar{n} = \bar{n} - \sum P_n$ ($n$ mod 3). Calculations for $k_B T/U = 1, 0.5, 0.3, 0.2$, and 0 are plotted in Fig. 3(d). For $\bar{n} < 2.5$, all curves show smaller loss than does the Poisson model. An insulator at lower temperature experiences fewer losses because thermal fluctuation is

reduced. At zero temperature, loss only occurs at $\bar{n} > 2$, where the occupancy $n \geq 3$ is unavoidable.

Surprisingly, our loss measurements do not follow the model with a uniform temperature for up to 800 ms hold time. Using $U = k_B \times 26$ nK and describing the deviation from a constant temperature contour by an effective local temperature $T_{\mathrm{eff}}(r)$, we find the center of the cloud has a lower $T_{\mathrm{eff}} \sim 6$ nK, while for the wing $T_{\mathrm{eff}} \sim 20$ nK even after 800 ms of hold time. This persistent temperature variation across the sample suggests that the heat flow is insufficient to establish a global thermal equilibrium even after 800 ms hold time. This may be aggravated by a large heat capacity of the atoms in the wing.

Both the slow mass and heat flows observed in this work raise the issue of describing quantum gases in optical lattices using a thermodynamic model. We suspect that the slow dynamics is partially due to our large sample size of $(100 \text{ sites})^2$ and the dimensionality of our system, and partially associated with the critical behavior of the system. Across the SF-MI transition, the sample enters the quantum critical regime, where long equilibration times are expected [16,28]. Other interesting mechanisms include the long lifetime of the excited doublon [13], which could slow down statistical redistribution of occupancies while supporting mass transport. Moreover, the slow recombination loss preferentially removes atoms at the center of the sample, creating $\sim 20\%$ observed reduction in the mean occupancy during 800 ms of hold time, which could lead to a radial temperature gradient assuming sufficient local rethermalization.

In summary, we show that the *in situ* density profiles of atoms in a 2D optical lattice provide a viable tool for investigating dynamic processes induced by chemical potential and temperature imbalance. In both cases, we find equilibration times much longer than the microscopic tunneling time scale. Further investigation into these processes and the relevance of our observation to the quantum dynamics in the critical regime will be reported in the future.

---

[1] I. Bloch, J. Dalibard, and W. Zwerger, Rev. Mod. Phys. **80**, 885 (2008).

[2] M. Lewenstein, A. Sanpera, V. Ahufinger, B. Damski, A. Sen, and U. Sen, Adv. Phys. **56**, 243 (2007).

[3] M. Greiner, O. Mandel, T. Esslinger, T. W. Hänsch, and I. Bloch, Nature (London) **415**, 39 (2002).

[4] S. Trotzky, L. Pollet, F. Gerbier, U. Schnorrberger, I. Bloch, N. V. Prokof'ev, B. Svistunov, and M. Troyer, arXiv:0905.4882.

[5] I. B. Spielman, W. D. Phillips, and J. V. Porto, Phys. Rev. Lett. **100**, 120402 (2008).

[6] M. P. A. Fisher, P. B. Weichman, G. Grinstein, and D. S. Fisher, Phys. Rev. B **40**, 546 (1989).

[7] D. Jaksch, C. Bruder, J. I. Cirac, C. W. Gardiner, and P. Zoller, Phys. Rev. Lett. **81**, 3108 (1998).

[8] R. Jördens, N. Strohmaier, K. Günter, H. Moritz, and T. Esslinger, Nature (London) **455**, 204 (2008).

[9] U. Schneider, L. Hackermüller, S. Will, Th. Best, I. Bloch, T. A. Costi, R. W. Helmes, D. Rasch, and A. Rosch, Science **322**, 1520 (2008).

[10] J. Hubbard, Proc. R. Soc. A **276**, 238 (1963).

[11] T. Kinoshita, T. R. Wenger, and D. S. Weiss, Nature (London) **440**, 900 (2006).

[12] K. Winkler, G. Thalhammer, F. Lang, R. Grimm, J. Hecker Denschlag, A. J. Daley, A. Kantian, H. P. Büchler, and P. Zoller, Nature (London) **441**, 853 (2006).

[13] N. Strohmaier, D. Greif, R. Jördens, L. Tarruell, H. Moritz, T. Esslinger, R. Sensarma, D. Pekker, E. Altman and E. Demler, Phys. Rev. Lett. **104**, 080401 (2010).

[14] E. Altman, A. Polkovnikov, E. Demler, B. I. Halperin, and M. D. Lukin, Phys. Rev. Lett. **95**, 020402 (2005).

[15] J. Mun, P. Medley, G. K. Campbell, L. G. Marcassa, D. E. Pritchard, and W. Ketterle, Phys. Rev. Lett. **99**, 150604 (2007).

[16] B. Damski, Phys. Rev. Lett. **95**, 035701 (2005); F. M. Cucchietti, B. Damski, J. Dziarmaga, and W. H. Zurek, Phys. Rev. A **75**, 023603 (2007).

[17] C.-L. Hung, X. Zhang, N. Gemelke, and C. Chin, Phys. Rev. A **78**, 011604(R) (2008).

[18] N. Gemelke, X. Zhang, C.-L. Hung, and C. Chin, Nature (London) **460**, 995 (2009).

[19] T. Kraemer, M. Mark, P. Waldburger, J. G. Danzl, C. Chin, B. Engeser, A. D. Lange, K. Pilch, A. Jaakkola, H.-C. Nägerl, and R. Grimm, Nature (London) **440**, 315 (2006).

[20] S. R. Clark and D. Jaksch, Phys. Rev. A **70**, 043612 (2004).

[21] T. Gericke, F. Gerbier, A. Widera, S. Fölling, O. Mandel, and I. Bloch, J. Mod. Opt. **54**, 735 (2007).

[22] This procedure suppresses systematic distortions of the density measurement. In previous works [18,23], our imaging was performed at low magnetic fields, where recombination and radiative losses preferentially reduce the density at the center and can enhance the plateau feature in deep lattices.

[23] C.-L. Hung, X. Zhang, N. Gemelke, and C. Chin, arXiv:0910.1382v1.

[24] B. Capogrosso-Sansone, Ş. G. Söyler, N. Prokofev, and B. Svistunov, Phys. Rev. A **77**, 015602 (2008).

[25] At $V_f = 13E_R$ and scattering length $a = 200a_0$, three-body loss rate for 3 atoms per site is $\sim 0.4 \text{ s}^{-1}$.

[26] T.-L. Ho and Q. Zhou, Phys. Rev. Lett. **99**, 120404 (2007).

[27] F. Gerbier, Phys. Rev. Lett. **99**, 120405 (2007).

[28] J. Zakrzewski and D. Delande, Phys. Rev. A **80**, 013602 (2009).